



Cite this: *RSC Adv.*, 2019, 9, 620

A water-stable luminescent metal–organic framework for effective detection of aflatoxin B1 in walnut and almond beverages†

Zhishang Li,^{‡a} Xiahong Xu,^{‡b} Yingchun Fu,^a Yuna Guo,^b Qi Zhang,^a Qiaoyan Zhang,^b Hua Yang^{*b} and Yanbin Li^{id*ac}

Sensitive and rapid detection of aflatoxin B1 (AFB1) without using antibody or biomolecular modifications in water is achieved using a novel water-stable luminescent metal–organic framework (LMOF) termed Zr-CAU-24. The 1,2,4,5-tetrakis(4-carboxyphenyl) benzene (H₄TCPB)-based LMOF with high water-stability has demonstrated drastic fluorescence fading in the presence of AFB1. The detection limit for AFB1 using this porous nanomaterial reaches as low as 19.97 ppb (64 nM), which is below the applicable action level for peanut and corn products set by the FDA and among the most sensitive sensors reported for AFB1. We further investigated its response to five other mycotoxins including AFB2, AFG1, AFG2, AFM and OTA and their Stern–Volmer quenching efficiencies are significantly below that of AFB1 (138 461 M⁻¹). The prepared water-stable LMOF was directly used for the detection of AFB1 in spiked walnut and almond beverages. High recovery rates (91–108%) were achieved in 5 min. We found that the quenching of H₄TCPB molecules towards mycotoxins was remarkably enhanced by anchoring them into the periodic framework and its mechanism was discussed. The presented method with acceptable detection limit is of potential for the development of low-cost, robust and sensitive sensors for the rapid detection of AFB1 in agricultural and food products.

Received 19th September 2018
 Accepted 2nd December 2018

DOI: 10.1039/c8ra07804a

rsc.li/rsc-advances

Introduction

Mycotoxins are secondary metabolites produced by *Aspergillus* that are frequently found in spoiled agricultural commodities (such as peanuts, corns, rice, and milk), posing significant adverse health effects worldwide.¹ Among them, aflatoxins (AFs) and ochratoxin A (OTA) represent the most dominant and harmful mycotoxins,² which have been proved teratogenic, mutagenic, and carcinogenic to human beings and animals.³ There are basically four types of AFs: B1, B2, G1, and G2 and AFB1 represents the most harmful one. In many countries, legislative limits were set for AFB1 in foodstuffs.⁴ More importantly, AFB1 has demonstrated high chemical stability against elevated temperature through food processing, making the prevention of their entrance into the food supply chain difficult. Therefore, it is extremely important to detect their

contamination at low concentration to ensure global food safety.⁵ Nowadays, there are basically two methods for the detection of AFs: enzyme-linked immunoassays and chromatographic-based methods, including high performance liquid chromatography (HPLC) and immunoassay chromatography.⁶ The former method provides a potable and rapid method for mycotoxins detection. However, low sensitivity and complex operation procedures has hampered its practical applications.⁷ Chromatographic-based methods are considered as facile, sensitive and portable sensing method for AFs sensing.⁸ Nevertheless, this method has some drawbacks such as high-cost, technique required operation and time-consuming sample preparation process. The incorporation of biomolecules in immunoassay chromatography also makes this method less robust. Thus, development of sensitive, low-cost and robust sensing methods for AFB1 is in high demand, especially in developing countries.⁹ Metal–organic frameworks (MOFs), as an emerging class of porous materials with high surface area, flexible chemical properties, rich functionalities and tuneable pore structures, have demonstrated great potential in the detection of harmful residues, especially for small molecules.^{10,11} For example, a series of luminescent Zr-based highly luminescent metal–organic frameworks (LOMF) were reported as sensitive chemical sensors for toxic chemicals detection and removal, including nitroaromatic explosives.^{12–15} Two water-stable 3D fluorescent Zr(IV)-based metal–organic

^aCollege of Biosystems Engineering and Food Science, Zhejiang University, 866 Yuhangtang Road, Hangzhou, 310058, China. E-mail: yanbinli@zju.edu.cn

^bState Key Lab Breeding Base for Zhejiang Sustainable Plant Pest Control, Institute of Quality and Standard for Agro-products, Zhejiang Academy of Agricultural Sciences, Hangzhou 310021, China

^cDepartment of Biological and Agricultural Engineering, University of Arkansas, Fayetteville, AR 72701, USA

† Electronic supplementary information (ESI) available. See DOI: 10.1039/c8ra07804a

‡ These two authors contributed equally to this work.



frameworks were constructed with different pore structures.¹⁶ Both their fluorescence could be efficiently quenched with nitro compound, which enables the sensitive detection of organic explosives with the detection limit reaches as low as ppb level. 2D Cd-based LMOF was also reported for the selective detection of nitroaromatic explosives different $-\text{NO}_2$ groups.¹⁷ Furthermore, a LMOF-based method was reported for TNP selective detection with the presence of other nitro compounds based on the specific electrostatic interaction and electron and energy transfer between TNP and LMOF.¹² Taking advantage of the cation-exchange approach, a water-stable Eu-MOF was explored as sensitive and selective Fe^{3+} sensor with potential applications in biological system.¹⁸ However, their potential as mycotoxins sensors was seldom investigated. Li *et al.* reported a highly sensitive Zn-based luminescent MOF (LMOF) towards mycotoxins that achieves a low detection limit of AFB1 (46 ppb) in 10 min. This novel sensing material is of potential for the development of applicable low-cost, rapid and sensitive mycotoxin sensors.¹⁹ However, Zn-based MOFs suffered from poor water-stability due to the fragile Zn–O bond under the attack of H_2O molecules,²⁰ which has generally limited its applications in industrial practices, such as water purification and sensing. Here, we present a robust Zr_6 -cluster based water-stable LMOF termed Zr-CAU-24 with sensitive response to AFs. With water-stable Zr^{4+} clusters and luminescent TCPB^{4-} severing as second building units (SBU) and organic linkers, respectively, the prepared Zr-CAU-24 nanocrystals have demonstrated high structure stability in water due to their strong metal-ligand bond strength.^{20–23} As-prepared Zr-LMOF crystals not only demonstrated high surface area but also revealed improved sensitivity towards AFB1 compared to free standing H_4TCPB molecules in water. The limit of detection reaches as low as 19.97 ppb in 5 min, which is below the applicable action level set by Food and Drug Administration (FDA) for cottonseed meals intended for beef cattle (300 ppb) and corn and peanut products (20 ppb).^{24,25}

Results and discussion

Characterization

Water-stable luminescent Zr-CAU-24 was synthesized according to a reported research with modifications.²⁶ In this study, benzoic acid was used as structure modulator to control the crystal size and morphology of prepared nanocrystals. Without benzoic acid, amorphous colloid-like polymer that is formed by the aggregation of nano-Zr-CAU-24 crystals (~ 30 nm) is observed (Fig. S1†). Notably, we also found that the amorphous polymer has demonstrated negligible response towards AFB1. Thus, incorporating the H_4TCPB into the long-range order periodic structure is necessary for its sensitive response towards AFB1. The as-prepared Zr-CAU-24 crystals have demonstrated a rod-like morphology with a size of ~ 1 μm (Fig. 2A) with strong blue fluorescence. As shown in Fig. 1A, the Zr^{4+} are coordinated by eight carboxylate groups to form a C-centred orthorhombic arrangement cluster ($[\text{Zr}_6(\mu_3\text{-O})_4(\mu_3\text{-OH})_4]^{12+}$). The rest coordination sites at the Zr^{4+} ions are occupied by H_2O and OH^- molecules as mentioned in other Zr-based MOFs. As reported,



Fig. 1 Crystal structure of Zr-CAU-24 that is constructed from the $[\text{Zr}_6(\mu_3\text{-O})_4(\mu_3\text{-OH})_4]^{12+}$ clusters (A) and TCPB^{4-} molecules (B). Ball-stick models of Zr-CAU-24 crystals (C) and (D).

the clusters are further bridged by TCPB^{4-} linkers (Fig. 1B) in a SCU topology, giving rise to a porous framework with rhombic channels of $\sim 5.3 \times 10.5$ Å and $\sim 2.4 \times 3.5$ Å in diameter (Fig. 1C and D). For rapid and sensitive detection of mycotoxins in water, the structure stability of Zr-CAU-24 crystals in water is of great importance.

To prove its water-stability, the prepared Zr-CAU-24 crystals were immersed in water for 24 h before it is measured with Powder X-ray Diffraction (PXRD) and N_2 adsorption/desorption isotherm. As shown in Fig. 2B, the XRD peaks before and after water treatment are in good agreement, indicating the intact pore structure after long time of operation in water. The PXRD pattern is also retained after the loading of AFB1, which proves that the Zr-MOF structure was well kept after its quenching of fluorescence by AFB1. Similar results can be found in its N_2 adsorption/desorption isothermal curves before and after 24 h



Fig. 2 Scanning electron microscopy images of prepared Zr-CAU-24 crystals with different magnification times. Scale bar: 1 μm (A, inset). PXRD of Zr-CAU-24 crystals before and after water treatment and AFB1 absorption, (B) and N_2 adsorption/desorption isotherms (C) of Zr-CAU-24 crystals before and after 24 h water treatment. TGA result of as-prepared Zr-CAU-24 crystals (D).



water treatment (Fig. 2C). We found that the Brunauer–Emmett–Teller (BET) surface area remained, which again proves its intact pore structure during water treatment. The isothermal curve of Zr-CAU-24 is in good agreement with type I adsorption/de-adsorption isothermal curve, which implies the uniform microporous structure of prepared Zr-CAU-24. Further pore size distribution analysis directly revealed that most of the micropores have an aperture of 1 nm (Fig. 2C, inset). Larger micropores of ~ 2 nm with higher accessibility to mycotoxins can also be found. Thermal gravimetric analysis (TGA) was used to prove the thermal stability of Zr-CAU-24 (Fig. 2D). It first exhibited a weight loss of 3% in the temperature range 50–200 °C. Sequentially, further weight loss of 5% was observed between 200–420 °C (loss of internal solvent molecules). The decomposition of the thermal robust porous material starts at 420 °C with a total weight loss of $\sim 38\%$ after degradation. With good water and thermal stability (~ 420 °C), this robust sensing material is considered as an appropriate candidate for the development of low-cost, rapid and sensitive sensors for detection of mycotoxins.

Detection of mycotoxins

Mycotoxin detection was achieved by monitoring the PL signal fading of Zr-CAU-24 crystals after reacting with mycotoxins. We first determined the optimum LMOF dosage to harvest the highest FL fading by reacting with 50 μM AFB1 (Fig. S2†). When 50 $\mu\text{g mL}^{-1}$ LMOF was applied, highest FL fading of 83% was achieved, while both lower and higher LMOF dosage decreased FL fading (73%). Sequentially, we examined its performance in the detection of AFB1 by adding given amount of toxins to the solution containing 50 $\mu\text{g mL}^{-1}$ Zr-CAU-24 crystals. The strong blue-fluorescence-emission LMOF nanocrystals were significantly quenched in 5 min and the signal was monitored by a fluorimeter (Fig. 3A). Under the excitation of 340 nm

wavelength, the fading of fluorescence intensity at 410 nm (Zr-CAU-24) is correlated linearly with the logarithmic molar volume of toxins (eqn (1))

$$y = 0.379 + 0.320 \lg x \quad (r^2 = 0.991) \quad (1)$$

$$y = (F_0 - F)/F_0 \quad (2)$$

where y represents the relative fluorescence intensity, x represents the molar volume of AFB1, and F_0 and F is the intensity of fluorescence with and without toxins, respectively. Good linear relationship between relative fluorescence ($(F_0 - F)/F_0$) and the logarithm of toxic concentration ($>99\%$) is achieved for a wide range of toxin concentrations (0.075 to 25 μM), which is of advantage over its counterparts.²⁷ The detection limit reaches as low as 19.97 ppb ($S/N = 3$). The value of this detection limit is below the tolerant level of cottonseed meals intended for beef cattle (300 ppb) and corn and peanut products (20 ppb) (FDA) and among those of the most sensitive materials reported for AFB1 sensing. Furthermore, we applied the sensing material to the detection of other two aflatoxins (AFG1, AFM) and ochratoxin A (OTA). Drastic fluorescence quenching was also observed and the liner relationships were obtained as shown in the Fig. S3–S5.† They all demonstrated good linear relationship between relative fluorescence and the logarithm of toxic concentration ($>98\%$), ranging from 0.075 to 25 μM . Stern–Volmer quenching efficiency is used to describe its sensitivity towards different mycotoxins.

$$I_0/I = K_{sv}[Q] + 1 \quad (3)$$

where I_0 represents the initial emission peak of intensity, I is the emission peak intensity upon the addition of analyte, $[Q]$ is molar intensity upon the addition of analyte (quencher) and K_{sv} is the quenching efficiency, which is used to quantitatively evaluate the performance of Zr-CAU-24 as a mycotoxin sensor. As shown in Fig. 3C, this porous nanomaterial has demonstrated sensitive quenching effect towards four kinds of mycotoxins including AFB1, AFG1, AFM and OTA and the K_{sv} reaches 138 461, 50 793, 68 119, 53 149 M^{-1} , respectively. The K_{sv} for AFB1 is almost doubled compared with that for AFG1, AFM and OTA, indicating its higher selectivity toward AFB1. Stronger orbital overlap (π – π conjugation) between AFB1 and Zr-CAU-24 is reported responsible for the enhanced selectivity towards AFB1 compared with other kinds of mycotoxins.¹⁴ To better reveal the different responses of Zr-CAU-24 toward different mycotoxins, we treated the analyst with a fixed concentration (50 μM) of AFB1, AFB2, AFG1, AFG2, AFM and OTA (Fig. 3D). The fluorescence intensity at 380 nm dropped drastically after adding of mycotoxins. Obvious red shift was observed in all test samples, which is due to the fluorescent properties of mycotoxins under the excitation of 340 nm.

Walnut and almond beverages are common products made from nuts, exposing them to the risk of being contaminated by AFB1. Therefore, we further applied this sensing material to the direct detection of AFB1 in the spiked samples (Table 1). AFB1 of three different concentrations (0.1 μM , 1 μM , 10 μM) were



Fig. 3 Emission spectra of Zr-CAU-24 with the incremental addition of AFB1 in water, with toxin concentrations given from 0 to 50 μM (A). Linear relationship between $\lg C_{\text{AFB1}}$ and FL intensity. Inset: optical photo of fluorescent Zr-CAU-24 crystals in water (left) and water (right) (B). Stern–Volmer curves acquired at $\lambda_{\text{ex}} = 340$ nm and $\lambda_{\text{em}} = 410$ nm for AFB1, AFG1, AFM and OTA (C). FL intensity fading of Zr-CAU-24 towards 50 μM AFB1, AFB2, AFG1, AFG2, AFM and OTA (D).



Table 1 Recovery rates of AFB1 in spiked walnut and almond beverages using fluorescent Zr-CAU-24 crystals (HPLC method was used as comparison)

	Spiked amount (μM)	HPLC (μM)	Proposed method (μM)	Recovery (%)
Walnut beverage	0.1	0.102	0.0975	98%
	1.0	1.007	1.079	108%
	10.0	9.969	9.73	97%
Almond beverage	0.1	0.0946	0.0966	97%
	1.0	0.956	1.041	104%
	10.0	9.73	9.06	91%

tested with Zr-CAU-24 and HPLC method is valued as a control to evaluate the recovery rates in real samples (Fig. S7†). High recoveries were achieved in all samples (91–108%), which is comparable to that of HPLC (95–102%). At low toxin concentration (0.1 μM), the recovery rates for walnut and almond beverages both reached 93%. It's noticed that this sensing method has demonstrated a wide liner range of 0.075–25 μM , while most of reported methods have narrow liner ranges.^{28–30} These results have revealed the potential of this water-stable sensing material for the development of low-cost, rapid, and potable mycotoxin sensors.

Mechanism of mycotoxin detection

By anchoring the fluorophore into the framework, the absorption wavelength presents a red shift from 280 nm to 330 nm (Fig. 4A) due to the strong π - π interaction in the framework, which is observed in other sensing materials reported. However, the emission wavelength of TCPB⁴⁻ remained at 410 nm (Fig. 4B), which implies a higher energy transfer efficiency in Zr-CAU-24 crystals. TCPB⁴⁻ is a strong fluorophore, but it has no strong interaction with AFs (Fig. 4C). Also, nano-Zr-CAU-24 crystals of ~ 30 nm demonstrates negligible fluorescence quenching effect towards AFB1. Thus, incorporating the fluorophore into a long-range order structure of metal-organic framework is essential for sensitive and selective quenching of AFB1. The quenching mechanism of LMOF as a mycotoxin sensor was due to the electron transfer between the LMOF and mycotoxins because the LUMO energy state of MOF is above the LUMO state of mycotoxins.¹⁹ However, the enhanced quenching efficiency of anchored TCPB⁴⁻ molecules in the Zr-CAU-24 was barely discussed. N₂ absorption/desorption curve demonstrates that the average pore size slightly decreases from 1 nm to 0.8 nm, which demonstrates that most pores of Zr-MOF is not occupied after AFB1 adsorption. Combined with the absorption testing result (Fig. S6†), it is found that the AFB1 was fully absorbed by the Zr-CAU-24 crystals and removed from the solution after sensing and the notable enhancement may be due to the amplified luminescence quenching of luminescent MOFs at the surface. The periodic structure of phosphorescent Zr-CAU-24 has allowed for long distance transfer of intra-MOF energy, which significantly enhances the electron-transfer quenching of fluorescence Zr-CAU-24 at the surface³¹ and thereby causes higher quenching efficiency of micron level Zr-CAU-24 crystals compared with nano-Zr-CAU-24 of ~ 30 nm.

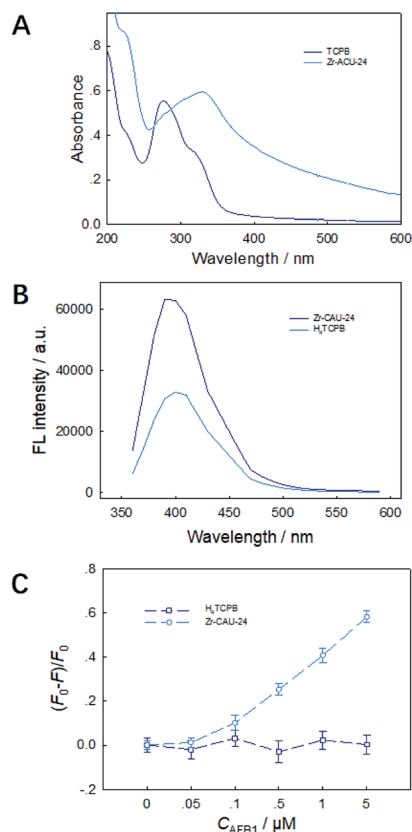


Fig. 4 UV-visible spectrum (A) and emission spectra ($\lambda_{\text{em}} = 410$ nm) (B) of TCPB⁴⁺ molecules and Zr-CAU-24 crystals. FL intensity fading of Zr-CAU-24 crystals and TCPB⁴⁺ molecules with the existence of AFB1 (C).

Experimental

Instrumentation

Hitachi SU-8000 field-emission electron scanning microscope (Hitachi, Japan) was used to characterize the morphology and the EDS of MOF particles with an acceleration voltage of 3 kV (10 nm gold coating). Powder X-ray Diffraction was conducted on an X' Pert PRO diffractometer (PANalytical, Netherland) equipped with Cu K α radiation ($\lambda = 0.15406$ nm) (scan speed: 1°min^{-1} ; 2θ range: 2 – 50° ; step size: 0.05°). The BET surface area of the MOF particles was measured using an AUTOSORB-1-C surface area and pore size analyzer (Quantachrome, USA) with samples degassed at 200°C for 24 h in advance. The thermal



- 3 M. Edite Bezerra da Rocha, F. da C. O. Freire, F. Erlan Feitosa Maia, M. Isabel Florindo Guedes and D. Rondina, *Food Control*, 2014, **36**, 159–165.
- 4 F. and A. O. of the U. Nations, *FAO Food and Nutrition Paper 81*, 2004.
- 5 A. G. Marroquin-Cardona, N. M. Johnson, T. D. Phillips and A. W. Hayes, *Food Chem. Toxicol.*, 2014, **69**, 220–230.
- 6 S. Yue, X. Jie, L. Wei, C. Bin, W. Dou Dou, Y. Yi, L. QingXia, L. JianLin and Z. TieSong, *Anal. Chem.*, 2014, **86**, 11797–11802.
- 7 L. Yang and R. Bashir, *Biotechnol. Adv.*, 2008, **26**, 135–150.
- 8 N. V. Beloglazova, E. S. Speranskaya, A. Wu, Z. Wang, M. Sanders, V. V. Gofman, D. Zhang, I. Y. Goryacheva and S. De Saeger, *Biosens. Bioelectron.*, 2014, **62**, 59–65.
- 9 G. S. Shephard, *Food Addit. Contam., Part A: Chem., Anal., Control, Exposure Risk Assess.*, 2008, **25**, 146–151.
- 10 Z. Hu, B. J. Deibert and J. Li, *Chem. Soc. Rev.*, 2014, **43**, 5815–5840.
- 11 H. Furukawa, K. E. Cordova, M. O’Keeffe and O. M. Yaghi, *Science*, 2013, **341**, 1230444.
- 12 S. S. Nagarkar, B. Joarder, A. K. Chaudhari, S. Mukherjee and S. K. Ghosh, *Angew. Chem., Int. Ed. Engl.*, 2013, **52**, 2881–2885.
- 13 S. S. Nagarkar, A. V. Desai and S. K. Ghosh, *Chem. Commun.*, 2014, **50**, 8915–8918.
- 14 S. Xie, H. Wang, Z. Liu, R. Dai and L. Huang, *RSC Adv.*, 2015, **5**, 7121–7124.
- 15 N. S. Bobbitt, M. L. Mendonca, A. J. Howarth, T. Islamoglu, J. T. Hupp, O. K. Farha and R. Q. Snurr, *Chem. Soc. Rev.*, 2017, **46**, 3357–3385.
- 16 B. Wang, X.-L. Lv, D. Feng, L.-H. Xie, J. Zhang, M. Li, Y. Xie, J.-R. Li and H.-C. Zhou, *J. Am. Chem. Soc.*, 2016, **138**, 6204–6216.
- 17 S. R. Zhang, D. Y. Du, J. S. Qin, S. J. Bao, S. L. Li, W. W. He, Y. Q. Lan, P. Shen and Z. M. Su, *Chem.–Eur. J.*, 2014, **20**, 3589–3594.
- 18 S. Dang, E. Ma, Z.-M. Sun and H. Zhang, *J. Mater. Chem.*, 2012, **22**, 16920–16926.
- 19 Z. Hu, W. P. Lustig, J. Zhang, C. Zheng, H. Wang, S. J. Teat, Q. Gong, N. D. Rudd and J. Li, *J. Am. Chem. Soc.*, 2015, **137**, 16209–16215.
- 20 H. Jasuja, N. C. Burtch, Y. G. Huang, Y. Cai and K. S. Walton, *Langmuir*, 2013, **29**, 633–642.
- 21 N. C. Burtch, H. Jasuja and K. S. Walton, *Chem. Rev.*, 2014, **114**, 10575–10612.
- 22 J. H. Cavka, S. Jakobsen, U. Olsbye, N. Guillou, C. Lamberti, S. Bordiga and K. P. Lillerud, *J. Am. Chem. Soc.*, 2008, **130**, 13850–13851.
- 23 D. Feng, Z.-Y. Gu, J.-R. Li, H.-L. Jiang, Z. Wei and H.-C. Zhou, *Angew. Chem.*, 2012, **124**, 10453–10456.
- 24 USFDA, *CPG Sec. 570.375 Aflatoxin in Peanuts and Peanut Products*, 2015.
- 25 USFDA, *CPG Sec. 683.100 Action Levels for Aflatoxins in Animal Feeds*, 2015.
- 26 M. Lammert, H. Reinsch, C. A. Murray, M. T. Wharmby, H. Terraschke and N. Stock, *Dalton Trans.*, 2016, **45**, 18822–18826.
- 27 Y. Xu, B. Chen, Q. He, Y. Lou Qiu, X. Liu, Z. He and Z. Xiong, *Anal. Chem.*, 2014, **86**, 8433–8440.
- 28 W. Xu, Y. Xiong, W. Lai, Y. Xu, C. Li and M. Xie, *Biosens. Bioelectron.*, 2014, **56**, 144–150.
- 29 J. C. Vidal, L. Bonel, A. Ezquerro, S. Hernández, J. R. Bertolín, C. Cubel and J. R. Castillo, *Biosens. Bioelectron.*, 2013, **49**, 146–158.
- 30 S. Piermarini, L. Micheli, N. H. S. Ammida, G. Palleschi and D. Moscone, *Biosens. Bioelectron.*, 2007, **22**, 1434–1440.
- 31 C. A. Kent, D. Liu, T. J. Meyer and W. Lin, *J. Am. Chem. Soc.*, 2012, **134**, 3991–3994.

